Combust. Sci. and Tech., 174(11&12): 205–222, 2002
Copyright © 2002 Taylor & Francis
0010-2202/02 $12.00 + .00
DOI: 10.1080/00102200290021632

MECHANISTIC PATHWAYS TO EXPLAIN H/C RATIO OF SOOT PRECURSORS

A. VIOLI* AND A. F. SAROFIM

Department of Chemical and Fuels Engineering, University of Utah, Salt Lake City, Utah, USA

T. N. TRUONG

Henry Eyring Center forTheoretical Chemistry, Department of Chemistry, University of Utah, Salt Lake City, Utah, USA

Pathways for the growth of high-molecular-mass compounds are presented, showing how reactions between aromatic moieties can explain recent experimental findings. A fundamental molecular analysis of polycyclic aromatic hydrocarbon growth processes in combustion systems involving five-membered ring compounds is presented using quantum mechanical density functional methods. Higher aromatics are produced through a two-step radical-molecule addition reaction and the iteration of this mechanism followed by rearrangement of the carbon framework ultimately leads to high-molecular-mass compounds. The distinguishing features of the proposed model lie in the chemical specificity of the routes considered. Naphthalene and acenaphthylene are used as examples of the aromatic and cyclopenta-fused aromatic classes of compounds postulated to be of importance in molecular weight growth. These reaction pathways are analyzed with a view

Accepted 29 May 2002.

This research is funded by the University of Utah Center for the Simulation of Accidental Fires and Explosions (C-SAFE), funded by the Department of Energy, Lawrence Livermore National Laboratory, under subcontract B341493. Additional support was provided by the University of Naples "Federico II," Department of Chemical Engineering. The calculations presented in this article were carried out at the Utah Center for High Performance Computing, University of Utah, which we acknowledge for computer time support.

*Address correspondence to violi@eng.utah.edu

toward explaining recent experimental findings on H/C ratio, NMR, and LMMS of soot precursors.

Keywords: soot precursors, formation pathways, H/C ratio

INTRODUCTION

In recent years great efforts have been undertaken to separate as many substances as possible from combustion exhaust and to determine their chemical structure (Homann et al., 1984). The main motive for this was to assess the pollution hazards of the polycyclic aromatic compounds, measure their concentrations, and determine their biological activities in different test systems. The larger part of the soluble substances belongs to the group of polycyclic aromatic hydrocarbons (PAHs) and their derivatives (Kausch et al., 1981). A large number is still unknown (Ciajolo et al., 1996; D'Alessio et al., 1992, 2000; Homann and Wagner, 1967; Minutolo et al., 1998). The group of aromatic hydrocarbons begins with benzene but it is not sharply defined at the high-mass end. PAHs up to coronene with 7 rings have been measured in many flames. Microprobing combined with capillary gas chromatography and mass spectrometry permits separation of compounds up to 8 aromatic rings. Bulk sampling and liquid chromatography has extended that range to 11 rings, while PAHs with up to 21 rings have been separated by gel chromatography (Lee and Bartle, 1981). Although the absolute amount of PAH formed depends strongly on the fuel, equivalence ratio, burning conditions, and so on, the relative concentrations of these stable PAHs do not change very much. This has been confirmed for different systems such as laminar, premixed, turbulent diffusion flames, diesel engines, and other combustors (Bockhorn et al., 1983; Ciajolo et al., 1982, 1996). Frequently, naphthalene and acenaphthylene are the two principal PAHs found. Starting from acenaphthylene, the concentration of PAHs decreases rapidly with increased molecular weight, on average by one order of magnitude with every increase in mass of 60 to 80 amu, rather independent of their absolute concentrations and of the combustion source (Homann, 1984).

One interesting issue in the PAH growth process is the change in H content. The large majority of PAHs are molecules with a flat, two-dimensional carbon skeleton (Keller et al., 2000). A one-dimensional carbon chain is found with the polyynes, $C_{2n}H_2$. The fullerenes, C_{2n},

$n > 15$ have a closed three-dimensional hollow carbon cage. Another class of large particles is the so-called aromers (Bachmann et al., 1996). They have a three-dimensional structure composed of PAH parts. They are discussed as precursors of fullerenes in flames. The carbon structure of the different classes of particles is closely related to their hydrogen content. Pericondensed PAHs with open structure have a larger H content than circum-PAH or PAH with condensed five-membered rings. Polyynes, chains of carbons with only two hydrogen atoms, have an even lower H/C ratio per carbon number.

The question arises as to the variation of hydrogen content and, hence, structure of larger PAHs and how these fit into a model of PAH growth. This article answers this question and synthesizes information on the formation of low-molecular-weight organic compounds, their transformation to transparent high-molecular-weight compounds, and the carbonization of these compounds. New reaction pathways for the formation of high-molecular-mass compounds are analyzed using a molecular-level approach. Recent experimental findings obtained by Dobbins et al. (1998) at Brown University, Homann (Keller et al., 2000) in Darmstadt, and Pugmire (Solum et al., 1989) at the University of Utah are reviewed and provide support for the proposed pathways.

NUMERICAL COMPUTATION

The configurations of reactants as well as intermediates, transition states, and products have been optimized by using the hybrid density functional B3LYP method (i.e., Becke's three-parameter nonlocal exchange functional; Becke, 1992a, 1992b, 1993 with the nonlocal correlation function of Lee, Yang, and Parr with the 6-31G(d,p) basis set (Hebre et al., 1986). Vibrational frequencies of all species involved in the reaction were calculated using the optimized geometries at the B3LYP/6-31G(d,p) level and they were used for characterization of the stationary points and calculation of zero-point energy (ZPE) corrections. All the energies cited in the following discussion include ZPE corrections. The stationary points were identified by the number of imaginary frequencies (NIMF) with NIMF = 0 for a stable species and NIMF = 1 for a transition state. Each transition state was connected to the corresponding minima by visualization of the normal mode corresponding to the imaginary frequency. All the calculations have been performed by using the Gaussian 98 program (Frisch et al., 1998). Rate constants are calculated with the

web-based VKLAB tool (vklab) (Zhang and Truong, 2001) using the Transition State Theory (TST). The thermal rate coefficient is expressed as

$$k(T) = \kappa(T)\sigma \frac{k_B T}{h} \frac{Q^{\pm}(T)}{\Phi^{R}(T)} e^{\{-\Delta V^{\pm}/k_B T\}}$$

where κ is the transmission coefficient accounting for the quantum mechanical tunneling effects, σ is the reaction symmetry number, $Q^{\pm}$ and Φ^{R} are the total partition functions of the transition state and of reactant per unit volume, respectively; $\Delta V^{\pm}$ is the classical barrier height; T is the temperature; k_B and h are the Boltzmann and Planck constants, respectively.

RESULTS

We previously introduced a model for the formation of high-molecular-mass compounds and soot (D'Anna and Violi, 1998; D'Anna et al., 2001; Violi et al., 1999), in which high-molecular-mass aromatic compounds are formed through reactive polymerization of small PAHs. The mechanism involves a sequence of chemical reactions between aromatic compounds with 6 π-electrons such as, benzene and naphthalene, and compounds containing conjugated double bonds such as, acenaphthylene and acephenanthrylene. The sequence begins with the H-abstraction from aromatic compounds to produce the corresponding radical (Violi et al., 2001a, 2001b)

$$Ar_1 + H = Ar_1^{*} + H_2 \quad (1)$$

which furnishes higher aromatics through a two-step radical-molecule reaction:

$$Ar_1^{*} + Ar_2\text{-}H = Ar_1\text{-}Ar_2\text{-}H \quad (2)$$

$$Ar_1\text{-}Ar_2\text{-}H + H = Ar_1\text{-}Ar_2 + H_2 \quad (3)$$

where Ar_1-Ar_2-H represents an intermediate formed through an addition reaction. Iteration of this mechanism followed by rearrangement of the carbon framework ultimately leads to the formation of high-molecular-mass compounds.

To add chemical specificity to these reaction pathways, a thorough analysis by means of density functional theory is reported. The reactants chosen for this study are naphthalene ($C_{10}H_8$) and acenaphthylene ($C_{12}H_8$). This choice is due both to the fact that these hydrocarbons are present in large concentrations in the PAH inventory and to the importance that PAHs with peripherally fused five-membered rings (CP-PAH), which include acenaphthylene, have in the flame-formation chemistry of soot (Benish et al., 1996; Frenklach, 1996; Frenklach and Ebert, 1988; Frenklach et al., 1998; Homann, 1989; McEnally and Pfefferle, 1998) and fullerenes (Lafleur et al., 1996).

Naphthalene is chosen as a representative of the Ar_1 class of compounds. The reaction rate for the H-abstraction by H atom has been calculated using TST. The Arrhenius parameters for the formation of 1* naphthyl via the reaction

$$C_{10}H_8 + H = 1*C_{10}H_7 + H_2$$

are $A = 1.1\text{E-}12$ (cm^3/mol-s), $n = 0.66$, $E/R = 5.51\text{E}3$ (K). On the basis of similarity of the reactants, the reaction is likely to follow a similar sequence to the reaction of benzene with H leading to the formation of the reactive phenyl radical, whose value was experimentally deduced in a shock-tube study by Kiefer et al. (1985). The differences between the experimental and calculated values is due to the fact that many H-abstraction reactions show upward curvature in their Arrhenius plots (Baulch et al., 1992; Tsang and Hampson, 1986) leading to appreciably higher rate coefficients at higher temperatures than one would estimate from a linear extrapolation of low-temperature measurements. Naphthyl radicals can also exist in the form 2-naphthyl, but 1-naphthyl is more stable and is the form selected here for analysis.

Acenaphthylene, chosen as a representative of an Ar_2 compound, is a fully conjugated PAH containing unsaturated five-membered rings externally fused to six-membered ring perimeters (CP-PAH). The reaction of 1-naphthyl and acenaphthylene, reaction (2), begins with the formation of the $C_{22}H_{15}$ species, reported in Figure 1 as Structure 1.

This intermediate is produced by the addition of naphthyl to the double bond of acenaphthylene. A π bond is broken and a σ bond is formed with a length of 1.52. Steric hindrance brings about distortions from planarity in the geometry. The barrier height for the new C-C bond formation is 0.23 kcal/mol (TS1). The energy of $C_{22}H_{15}$ at our B3LYP

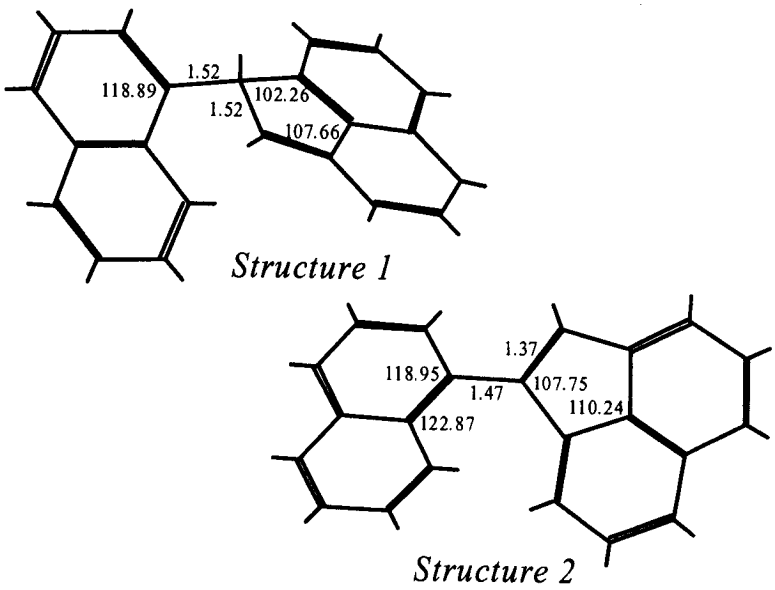

Figure 1. Optimized structures for the intermediate $C_{22}H_{15}$ (Structure 1) and $C_{22}H_{14}$ (Structure 2) at B3LYP level.

level is about 43 kcal/mol lower than that of the reactants. The unpaired electron is on the less substituted carbon in the five-membered ring. From this intermediate, it is possible to consider different pathways, that is, unimolecular β-scission reactions, but in a rich combustion environment high concentrations of H-atom are available so the intermediate can undergo an abstraction reaction. In particular, the H bonded to the sp^3 carbon in the 5-membered ring can be abstracted by H atoms present in the gas phase to obtain the product ($C_{22}H_{14}$) reported in Figure 1 as Structure 2. For the latter reaction, no transition state has been identified at the B3LYP level of theory. This means that if the transition state exists, its energetic barrier is within the uncertainty of the level B3LYP (4–5 kcal/mol). Because the energy of this transition state (if it exists) is well below that of initial reactants, as the intermediate is formed, it rapidly forms the products ($C_{22}H_{14} + H_2$), indicating that in the approximation of the steady state, the concentration of $C_{22}H_{15}$ is very low.

The two electrons on the carbons in the five-membered ring arrange themselves, giving back a double bond in the five-membered ring. H-abstraction is exothermic because of the restoration of the resonance structure. The energy is 107 kcal/mol lower than that of the reactants. The relief of steric overcrowding is accompanied by a flattening of molecular geometry and an increase of the stabilization through resonance. The reaction rate for the naphthyl and acenaphthylene addition reaction has been evaluated using TST and the calculated rate expression is

$$k(T) = 7.83 * T^{3.42} \exp(-91.56/T) \ (\mathrm{cm}^3/\mathrm{mol\text{-}s})$$

The accuracy of the B3LYP method has been reported by several research groups (Richter et al., 2001; Zhang and Truong, 2000).

The equilibrium constant between reactants (naphthyl and acenaphthylene) and products ($C_{22}H_{14} + H_2$) has been evaluated using The Rate code and the result is reported in Figure 2.

The reaction between 1-naphthyl and acenaphthylene presents a negative ΔS: the system loses six degrees of freedom (three translations and three rotations). During the reaction $C_{22}H_{15} + H = C_{22}H_{14} + H_2$ the system gets two rotations for the formation of the linear molecule H_2 and

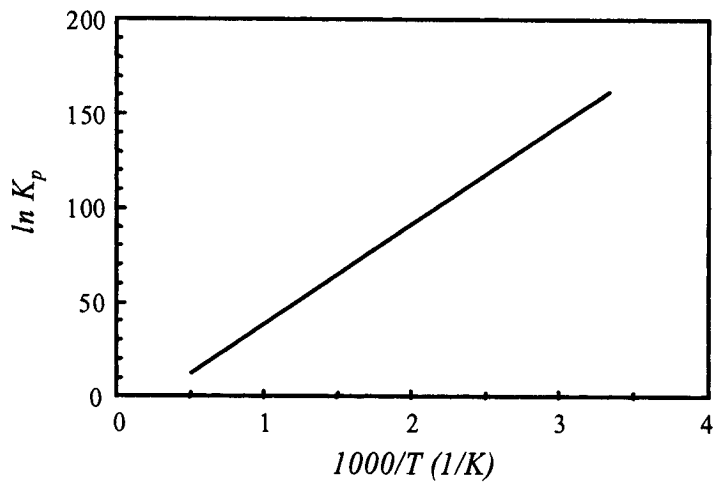

Figure 2. Predicted equilibrium constant between reactants ($C_{10}H_7 + C_{12}H_8$) and products ($C_{22}H_{14} + H_2$).

ΔS is positive. The equilibrium constant approaches 1 ($\Delta G = 0$) for $T \sim 2000$ K. H-abstraction from Structure 1 is necessary to get resonant-stable compounds such as $C_{22}H_{14}$. Without this added reaction Structure 1 would decompose to the reactants: The decrease in entropy in polymerization at high temperatures needs to be offset by the ΔH resulting from the H-abstraction to provide a favorable ΔG for the forward reaction.

The relative energy ΔE (kcal/g) diagram for this mechanism is reported in Figure 3. The reference value considered for this diagram is represented by the sum of the contribution of naphthyl, acenaphthylene, and H atom, the latter being involved in the H-abstraction reactions.

The reactions just described represent the first step of a sequence of reactions that can be easily repeated. For example, $C_{22}H_{14}$ can undergo H-abstraction to produce the corresponding radical that then produces $C_{34}H_{21}$ through addition reaction with acenaphthylene. The latter can lose the H bonded to the sp^3 C in the five-membered ring and produce $C_{34}H_{20}$, whose optimized geometry at the B3LYP/6-31G(d,p) level is reported in Figure 4.

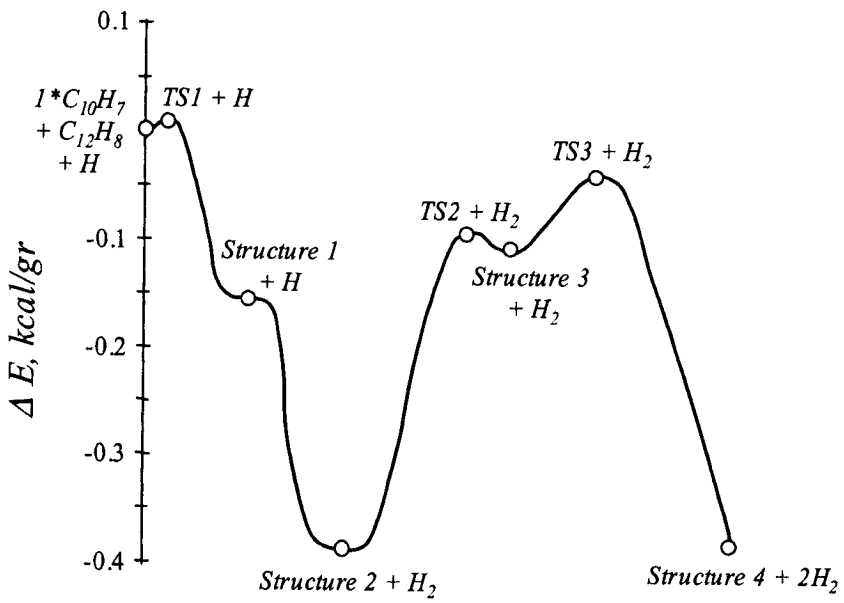

Figure 3. Potential energy diagram at the B3LYP/6-31G(d,p) level.

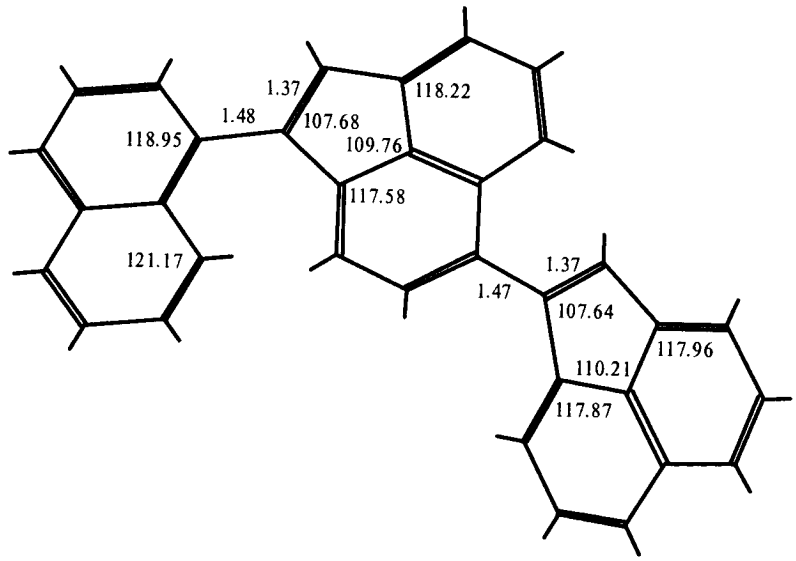

Figure 4. Optimized structure for the intermediate $C_{34}H_{21}$ (Structure 3) at the B3LYP level.

In this scenario, soot inception consists in the progressive aromatization of the structures through dehydrogenation. The abstraction of H atoms creates additional double bonds and, consequently, fused aromatic rings in the cluster with the increased extension of aromatic islands inside the structure. Little is known about the mechanism of this type of reactions, namely, cyclodehydrogenation reactions. Two hydrogen atoms are lost, and a new ring is created by the creation of a new C-C bond. One possible pathway cyclodehydrogenation reaction that involves ring closure and H_2 elimination is reported in the following text.

A six-membered ring (Structure 3) is formed from $C_{22}H_{14}$ (Structure 2) through a transition state (TS2), which bonds C1 to C1′ (see Figure 5). The ring closure is endothermic by ca. 80 kcal/mol and its barrier is 100 kcal/mol. The connection between Structure 2–TS2–Structure 3 is confirmed by intrinsic reaction coordinate calculations.

From Structure 3 the reaction continues by elimination of H_2. The atoms H1 and H1′ are now both in the same plane and their distance is 1.9 Å. The second transition state (TS3) requires an energy of ca. 34 kcal/mol. The H1-C1 bond is 1.33 Å while the H1′-C1′ is 1.36. This is due to the different influence of the two aromatic parts (naphthyl and acenaphthyl) on H atoms. In the final configuration (Structure 4) the two

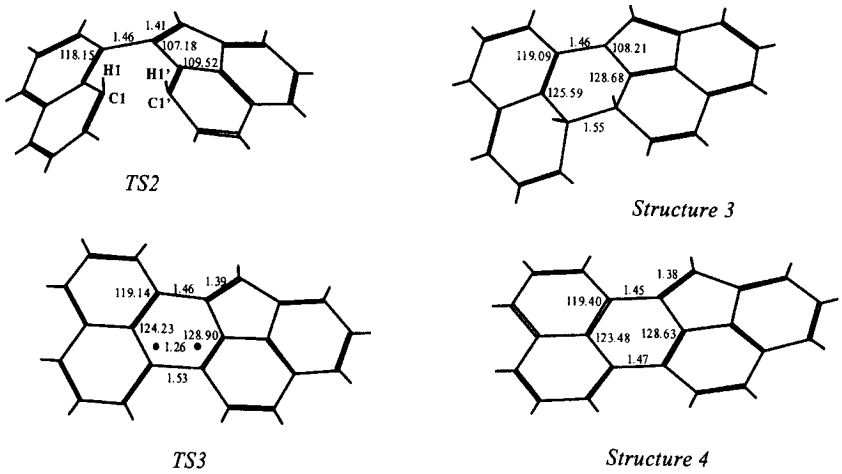

Figure 5. Optimized structures for TS2, Structure 3, TS3, and Structure 4 at the B3LYP level.

H atoms have been eliminated and the energy of product is 85 kcal/mol lower than the reactants. The energetic pathway is reported in Figure 5. A similar trend is expected for a ring-closure reaction starting from $C_{34}H_{20}$. In this case the relative energetic barriers will be smaller due to the more stable compounds formed. The energies for all the species are summarized in Table 1.

We used the Evans-Polanyi relationships to correlate the heat of reaction to the barrier energy for classes of reactions in order to extend this kinetic sequence to higher molecular masses and also to include different compounds that belong to the two classes of aforementioned aromatics. In this article we report results obtained for H-abstraction reactions from different aromatics by H atoms to form the corresponding radical and H_2, reaction (1). The results have been obtained using B3LYP/6-31G(d,p) method and are reported in Figure 6.

The circles show the relation for H-abstraction from the cyclopentafused PAH class, that is, acenaphthylene, aceanthrylene, acephenanthrylene, cyclopenta[cd]pyrene, and benzene, naphthalene, anthracene, and pyrene. To interpret this linear free-energy relationship we can use the Polanyi (Evans and Polanyi, 1936) relationship:

$$E_a = E_a^0 + \gamma_p \Delta H_r$$

Table 1. Relative energies (Z-P Energy-corrected, in kcal/g) for species involved in the reaction pathway (compounds named according to Figure 2)

Species	ZPE[a]	B3LYP/6-31G(d,p)[b]
$C_{10}H_7$	6.77E-1	0
$C_{12}H_8$	6.59E-1	0
H	0	0
TS1 + H	6.62E-1	8.29E-4
Str.1 + H	6.68E-1	−1.53E-1
Str.2 + H_2	6.67E-1	−3.82E-1
TS2 + H_2	6.60E-1	−9.80E-2
Str.5 + H_2	6.61E-1	−1.01E-1
TS3 + H_2	6.42E-1	−3.94E-2
Str.6 + $2H_2$	6.42E-1	−3.82E-1

[a]ZPE (kcal/g) calculated at B3LYP/6-31G(d,p) level.

[b]The total energies (in Hartree) for naphthyl, acenaphthylene, H atom, and H_2 are −385.2161474, −461.4052055, −0.5002728, and −1.1785393, respectively.

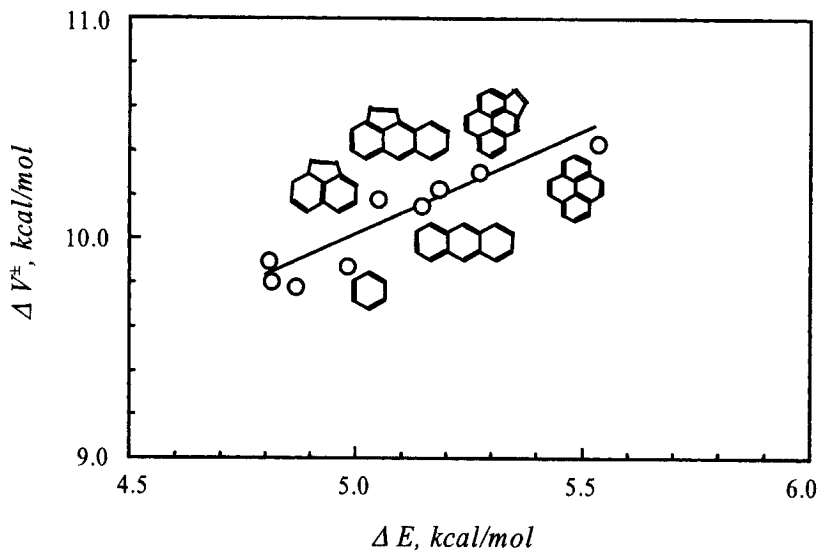

Figure 6. Activation barriers vs. heat of reaction of H-abstraction reactions from several compounds.

where E_a^0 is the intrinsic activation barrier and γ_p is the transfer coefficient. The basic implication of the Evans-Polanyi model is that activation barriers arises because of the Pauli repulsions and because of the bond scission and distortions that occur during reaction. Among the data reported in Figure 6 there is an approximately linear relationship between the heat of reaction and the activation barrier for the two classes of reaction

$$\Delta V^{\neq} = 0.975\Delta E + 5.144$$

and consequently the Polanyi relation is a quite useful way to correlate data. Note that if one can guess E_a^0 and γ_p one can predict activation barriers for a series of closely related elementary reactions.

DISCUSSION

The concept presented in this article of the linking of two-, three-aromatic rings in open structures that grow to yield high-molecular-mass compounds that subsequently dehydrogenate to form soot explains some important experimental observations.

H/C Ratio Data

If six-membered aromatic rings condense to form PAHs only by ortho-fused condensation (e.g., anthracene, phenanthrene) the series exhibits linear catenation. Such structures belong to the $C_{4n+2}H_{2n+4}$ family of PAHs. The molar ratio H/C approaches 0.5 in the limit as n becomes very large (Solum et al., 1989). Two-dimensional or circular catenation (e.g., coronene, circumcoronene) may also be considered for PAH with all other types of condensation falling between the structural limits defined by these two extremes. The ratio $H/C = 1/n$ approaches zero as the cluster grows. To calculate the aromatic cluster size, only linear catenation and circular catenation need to be considered (Solum et al., 1989). For a linear catenation it can be shown that

$$H/C = (2n + 4)/(4n + 2)$$

for a linear series index of

$$n = (C - 2)/4$$

where C is the number of carbon atoms in the aromatic cluster. The corresponding quantities for circular catenation are

$$H/C = 1/n$$

and the circular series index is

$$n = (C/6)^{0.5}$$

A plot of H versus C for linear and circular catenation is shown in Figure 7 as dashed and solid lines, respectively. Homann and coworkers (Keller et al., 2000) analyzed large PAH molecules and radicals in a low-pressure benzene-oxygen flame using molecular beam time-of-flight mass spectrometry and resonance-enhanced multiphoton ionization. They reported a C-H diagram for each molecular formula C_xH_y identified in flame, and their results are rearranged in Figure 7 and plotted as empty

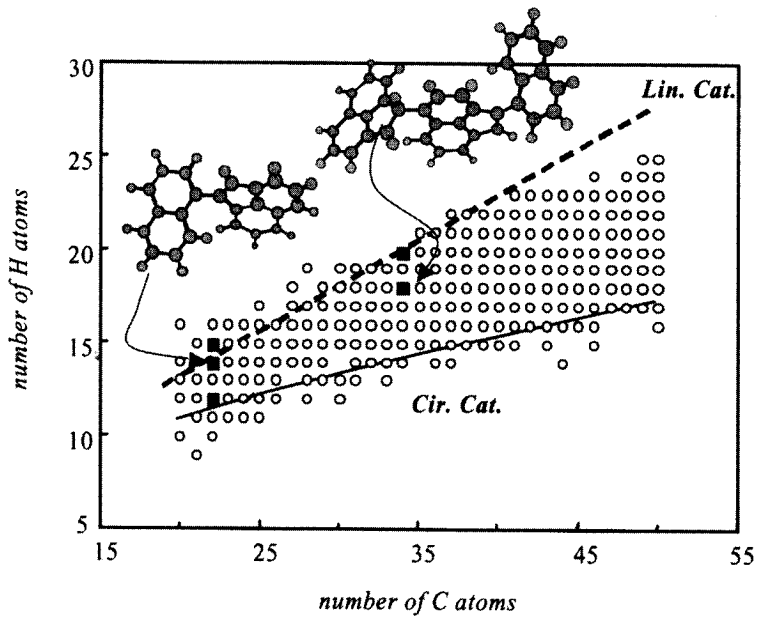

Figure 7. C-H diagram of PAHs and PAH radicals readapted by Keller et al. (2000). The dashed and solid lines represent the linear and circular catenation, respectively. The black squares mark the molecules studied in this article.

points. PAHs are found for every number of C atoms in the mass range studied (18–70 carbon atoms per molecule). The data show that the majority of PAHs are located between the two extremes of linear and circular catenation. The totality of points represent the ensemble of PAHs and PAH radicals with different molecular formulas. The formulas of six-ring PAHs with most pericondensed ring structures like coronene ($C_{24}H_{12}$), circumcoronene ($C_{54}H_{18}$), and so forth, lie on the solid line in the diagram. The authors showed that large H-rich PAHs (compounds described by a formula comprising data between the two lines) play a decisive role in reactions, both with respect to growth and consumption, irrespective of whether they are molecules or radicals. As most of the PAHs are of the pericondensed type, enriched hydrogen in their structure means more open structures with 4C bays or larger coves at which reactions might take place preferentially. The open structure obtained with the reaction scheme presented (black squares points) provides an explanation for the H/C ratios of soot precursors and young soots being much higher than those of polybenzenoid structures of equal molecular weight. Polyynes are not considered here since their H/C falls rapidly with n below the values of interest [$H/C = 1/(2n+1)$] but they can, as side chains, explain some of the data below the bounding lines.

LMMS Analysis Data

Dobbins and coworkers analyzed samples of soot precursor particles and carbonaceous soot from an ethene diffusion flame by means of laser microprobe mass spectrometry (LMMS). They found that three prominent masses, 252, 276, and 300 (ca. C20–C24), constitute 45% of the total population. The presence of this PAH triad as the dominant PAH components of the precursor particle material is consistent with other reports of the chemical composition of flame-generated soot from various gaseous and liquid fuels in diverse flame configurations (Benner et al., 1990; Olsen et al., 1987). In all of these studies, the 252–276–300 u species were found to coexist along with other PAHs in relatively large soot samples captured on a cold surface or by a filter medium for subsequent analysis by chromatography. The frequent occurrence of these species is evidence that the route to the formation of carbonaceous soot is through the intermediate 200–300 u PAH irrespective of the fuel composition or the nature of the combustion process. Fragments identified with carbon numbers of 16 to 36 (peak 20 or 22) correspond to two- three-ring

aromatic compounds or their dimers, which might be produced by the laser microprobe breaking some of the cross-links (Dobbins et al., 1998).

NMR Analyses

Solum et al. (1989) performed NMR measurement of young soots and their precursors formed by the injection of byphenyl and pyrene in flames and they showed open structures similar to those proposed in the current study. They showed that soot growth consists not only of ring-size growth but also cluster cross-linking, which could result in the formation of large cross-linked structures. The large number of cross-link sites per cluster suggests that a significant amount of cluster polymerization has occurred. This result can be also used to justify the new polymerization route and to quantify the cyclodehydrogenation reactions.

CONCLUSIONS

A fundamental molecular analysis of PAH growth processes in combustion systems involving five-membered ring compounds is presented using quantum mechanical density functional methods. A sequence of chemical reactions between aromatic compounds (e.g., naphthyl) and compounds containing conjugated double bonds (e.g., acenaphthylene) is studied in detail. The distinguishing features of the new reaction mechanism lie in the chemical specificity of the routes considered. The aromatic radical attacks the double bond of five-membered ring PAHs. This involves specific compounds that are exceptional soot precursors as they form resonantly stabilized radical intermediates, relieving part of the large strain in the five-membered rings by formation of linear aggregates. The concept presented in this article of the linking of two-, three-aromatic rings in open structures that grow to yield high-molecular-mass compounds that subsequently dehydrogenate to form soot explains the H/C ratios, LMMS analysis, and NMR results recently obtained by different research groups.

REFERENCES

Bachmann, M., Wiese, W., and Homann, K.-H. (1996) PAH and aromers: Precursors of fullerenes and soot. *Proc. Combust. Instit.*, **26**, 2259.

Baulch, D.L., Cobos, C.J., Cox, R.A., Esser, C., Frank, P., Just, T., Kerr, J.A., Pilling, M.J., Troe, J., Walker, R.W., and Warnatz, J. (1992) Evaluated kinetic data for combustion modeling. *J. Phys. Chem. Ref. Data*, **21**, 411.

Becke, A.D. (1992a) Density-functional thermochemistry. I. The effect of the exchange-only gradient correction. *J. Chem. Phys.*, **96**, 2155.

Becke, A.D. (1992b) Density-functional thermochemistry. II. The effect of the Perdew-Wang generalized-gradient correlation correction. *J. Chem. Phys.*, **97**, 9173.

Becke, A.D. (1993) Density-functional thermochemistry. III. The role of exact exchange. *J. Chem. Phys.*, **98**, 5648.

Benish, T.G., Lafleur A.L., Taghizadeh, K., and Howard, J.B. (1996) C_2H_2 and PAH as soot growth reactants in premixed C_2H_4-air flames. *Proc. Combust. Instit.*, **26**, 2319.

Benner, B.A., Bryner, N.P., Wise, S.A., Mulholland, G.W., Lao, R.C., and Fingas, M.F. (1990) Polycyclic aromatic hydrocarbon emissions from the combustion of crude oil on water. *Environ. Sci. Technol.*, **24**, 1418.

Bockhorn, H., Fetting, F., and Wenz, H.W. (1983) Investigation of the formation of high molecular hydrocarbons and soot in premixed hydrocarbon-oxygen flames. *Bunsen-Ges. Phys. Chem.*, **87**, 1067.

Ciajolo, A., Barbella, R., Mattiello, M., and D'Alessio, A. (1982) Axial and radial measurements of soot and PAH in a light oil flame. *Proc. Combust. Instit.*, **19**, 1369.

Ciajolo, A., D'Anna, A., Barbella, R., Tregrossi, A., and Violi, A. (1996) The effect of temperature on soot inception in premixed ethylene flames. *Proc. Combust. Instit.*, **26**, 2327.

D'Alessio, A., D'Anna, A, D'Orsi, A., Minutolo, P., Barbella, R., and Ciajolo, A. (1992) Precursor formation and soot inception in premixed ethylene flames. *Proc. Combust. Instit.*, **24**, 973.

D'Alessio, A., D'Anna, A., Minutolo, P., Sgro, L.A., and Violi, A. (2000) On the relevance of surface growth in soot formation in premixed flames. *Proc. Combust. Instit.*, **28**, 2547.

D'Anna, A. and Violi, A. (1998) A kinetic model for the formation of aromatic hydrocarbons in premixed laminar flames. *Proc. Combust. Instit.*, **27**, 425.

D'Anna, A., Violi, A., D'Alessio, A., and Sarofim, A.F. (2001) A reaction pathway for nanoparticle formation in rich premixed flames. *Combust. Flame* **127**, 1995.

Dobbins, R.A., Fletcher, R.A., and Chang, H.-C. (1998) The evolution of soot precursor particles in a diffusion flame. *Combust. Flame*, **115**, 285.

Evans, M.G. and Polanyi, M. (1936) Further considerations of the thermodynamics of chemical equilibria and reaction rates. *Trans. Faraday Soc.*, **32**, 1340.

Frenklach, M. (1996) On surface growth mechanism of soot particles. *Proc. Combust. Instit.*, **26**, 2285.

Frenklach, M. and Ebert, L.B. (1988) Comment on the proposed role of spheroidal carbon clusters in soot formation. *J. Phys. Chem.*, **92**, 561.

Frenklach, M., Moriarty, N.W., and Brown, N.J. (1998) Hydrogen migration in polyaromatic growth. *Proc. Combust. Instit.*, **27**, 1655.

Frisch, M.J., Trucks, G.W., Schlegel, H.B., Scuseria, G.E., Robb, M.A., Cheeseman, J.R., Zakrzewski, V.G., Montgomery, J.A., Stratmann, R.E., Jr., Burant, J.C., Dapprich, S., Millam, J.M., Daniels, A.D., Kudin, K.N., Strain, M.C., Farkas, O., Tomasi, J., Barone, V., Cossi, M., Cammi, R., Mennucci, B., Pomelli, C., Adamo, C., Clifford, S., Ochterski, J., Petersson, G.A., Ayala, P.Y., Cui, Q., Morokuma, K., Malick, D.K., Rabuck, A.D., Raghavachari, K., Foresman, J.B., Cioslowski, J., Ortiz, J.V., Baboul, A.G., Stefanov, B.B., Liu, G., Liashenko, A., Piskorz, P., Komaromi, I., Gomperts, R., Martin, R.L., Fox, D.J., Keith, T., Al-Laham, M.A., Peng, C.Y., Nanayakkara, A., Gonzalez, C., Challacombe, M., Gill, P.M.W., Johnson, B., Chen, W., Wong, M.W., Andres, J.L., Gonzalez, C., Head-Gordon, M., Replogle, E.S., and Pople, J.A. (1998) Gaussian 98, Revision A.7, Gaussian, Inc., Pittsburgh, PA.

Hebre, W., Radom, L., Schleyer, P.R., and Pople, J.A. (1986) *Ab Initio Molecular Orbital Theory*, Wiley, New York.

Homann, K.H. (1984) Formation of large molecules, particulates and ions in premixed hydrocarbon flames; progress and unresolved *questions*. *Proc. Combust. Instit.*, **20**, 857.

Homann, K.H. and Wagner, H.Gg. (1967) New aspects of the mechanism of carbon formation in premixed flames. *Proc. Combust. Instit.*, **11**, 371.

Kausch, W.J., Clampitt, C.M., Prado, G., Hites, R.A., and Howard, J.B. (1981) Nitrogen-containing polycyclic aromatic compounds in sooting flames. *Proc. Combust. Instit.*, **18**, 1097.

Keller, A., Kovacs, R., and Homann, K.-H. (2000) Large molecules, ions, radicals and small soot particles in fuel-rich hydrocarbon flames. Part IV. Large polycyclic aromatic hydrocarbons and their radicals in a fuel-rich benzene-oxygen flame. *Phys. Chem. Chem. Phys.*, **2**, 1667.

Kiefer, J.H., Mizerka, L.J., Patel, M.R., and Wei, H.-C. (1985) A shock tube investigation of major pathways in the high-temperature pyrolysis of benzene. *J. Phys. Chem.*, **89**, 2013.

Lafleur, A.L., Howard, J.B., Taghizadeh, K., Plummer, E.F., Scott, L.T., Necula, A., and Swallow, K.C. (1996) Identification of $C_{20}H_{10}$ dicyclopentapyrenes in flames: Correlation with corannulene and fullerene formation. *J. Phys. Chem.*, **100**, 17421.

Lee, M.L. and Bartle, K.D. (1981) The chemical analysis of particulate carbon. In D.C. Siegla, and G.W. Smith, (Eds.) *Particulate Carbon Formation During Combustion*, Plenum Press, New York, pp. 91–106.

McEnally, C.S. and Pfefferle, L.D. (1998) An experimental study in non-premixed flames of hydrocarbon growth processes that involve five-membered carbon rings. *Combust. Sci. Technol.*, **131**, 323.

Minutolo, P., Gambi, G., and D'Alessio, A. (1998) Properties of carbonaceous nanoparticles in flat premixed C_2H_4/air flames with C/O ranging from 0.4 to soot appearance limit. *Proc. Combust. Instit.*, **27**, 1461.

Olsen, K.L., Harris, S.J., and Weiner, A.M. (1987) Characterization of polycyclic aromatic hydrocarbons on soot from premixed flat flames. *Combust. Sci. Technol.*, **51**, 97.

Richter, H., Mazyar, O.A., Sumathi, R., Green, W.H., Howard, J.B., and Bozzelli, J.W. (2001) Detailed kinetic study of the growth of small polycyclic aromatic hydrocarbons. 1. 1-Naphthyl + ethyne. *J. Phys. Chem. A*, **105**, 1561.

Solum, M.S., Pugmire, R.J., and Grant, D.M. (1989) 13C solid-state NMR of argonne premium coals. *Energy Fuels*, **3**, 187.

Tsang, W. and Hampson, R.F. (1986) Chemical kinetic data base for combustion chemistry. Part 1. Methane and related compounds. *J. Phys. Chem. Ref. Data*, **15**, 1087.

Violi, A., D'Anna, A., and D'Alessio, A. (1999) Modeling of particulate formation in combustion and pyrolysis. *Chem. Eng. Sci.*, **54**, 3433.

Violi, A., Truong, T.N., D'Anna, A., D'Alessio, A., and Sarofim, A.F. (2001) Quantum Mechanic Study of High Molecular Mass Compounds in Combustion Conditions. *Proceedings of the 2nd Joint Meeting of the U.S. Sections of the Combustion Institute*, Oakland, CA, 25–28 March.

Violi, A., Truong, T.N., and Sarofim, A.F. (2001) Quantum mechanical study of molecular weight growth process by combination of aromatic molecules. *Combust. Flame*, **126**, 1506.

Zhang, S. and Truong, T.N. (2000) Thermal rate constants of the NO_2 fission reaction of gas phase a-HMX: A direct ab initio dynamics study. *J. Phys. Chem. A*, **104**, 7304.

Zhang, S. and Truong, T.N. (2001a) Virtual Kinetic Laboratory. http://vklab.hec.utah.edu (accessed September 2002).

Zhang, S. and Truong, T.N. (2001b) Branching ratio and pressure dependent rate constants of multichannel unimolecular decomposition of gas-phase a-HMX: An ab initio dynamics study. *J. Phys. Chem. A*, **105**, 2427.